Physica A 496 (2018) 162–170

Contents lists available at ScienceDirect

Physica A

journal homepage: www.elsevier.com/locate/physa

A network of networks model to study phase synchronization using structural connection matrix of human brain

F.A.S. Ferrari [a,*], R.L. Viana [b], A.S. Reis [b], K.C. Iarosz [c], I.L. Caldas [c], A.M. Batista [c,d]

[a] Universidade Federal dos Vales do Jequitinhonha e Mucuri, Instituto de Engenharia, Ciência e Tecnologia, Janaúba, MG, Brazil
[b] Universidade Federal do Paraná, Departamento de Física, Curitiba, PR, Brazil
[c] Universidade de São Paulo, Instituto de Física, São Paulo, SP, Brazil
[d] Universidade Estadual de Ponta Grossa, Departamento de Matemática e Estatística, Ponta Grossa, PR, Brazil

HIGHLIGHTS

- Here, chemical and electrical synapses are considered to describe a neural network.
- The network exhibits phase synchronization depending on the synaptic strength.
- Different functional structures are observed as synaptic strength is varied.
- The observed synchronization can be suppressed by appropriated feedback signals.
- The suppression of synchronization depends on feedback intensity and time delay.

ARTICLE INFO

Article history:
Received 20 June 2017
Received in revised form 4 November 2017
Available online 30 December 2017

Keywords:
Suppression of synchronization
Rulkov map
Control
Delay
Neural networks

ABSTRACT

The cerebral cortex plays a key role in complex cortical functions. It can be divided into areas according to their function (motor, sensory and association areas). In this paper, the cerebral cortex is described as a network of networks (cortex network), we consider that each cortical area is composed of a network with small-world property (cortical network). The neurons are assumed to have bursting properties with the dynamics described by the Rulkov model. We study the phase synchronization of the cortex network and the cortical networks. In our simulations, we verify that synchronization in cortex network is not homogeneous. Besides, we focus on the suppression of neural phase synchronization. Synchronization can be related to undesired and pathological abnormal rhythms in the brain. For this reason, we consider the delayed feedback control to suppress the synchronization. We show that delayed feedback control is efficient to suppress synchronous behavior in our network model when an appropriate signal intensity and time delay are defined.

1. Introduction

The cerebral cortex plays a key role in complex cortical functions, such as language, thought, perception, and memory [1]. It can be separated into areas according to their specific functions, known as cortical areas. Every cortical area is associated with one main function, such as process visual, taste, hearing, olfaction, and touch inputs or deliver motor commands [1]. One possibility for the emergence of specialized areas is the economic wiring. This way, it is easier for the brain to process information if the neurons that perform similar roles are closer [2]. The cortical areas are connected among themselves

* Corresponding author.
E-mail address: fabiano.ferrari@ufvjm.edu.br (F.A.S. Ferrari).

https://doi.org/10.1016/j.physa.2017.12.129
0378-4371/

through a complex pattern of connectivity [3]. The brain integrates the information from different cortical areas (and other brain areas) to produce a more complete information [4]. The interplay between the cortical areas and the complex structural network of the cerebral cortex produce the typical dynamical properties observed in the brain [5].

Neural synchronization in the cortex area can be observed in many species, for instance in humans, monkeys and cats [6]. Experimental evidences show that neural interactions can be modulated by means of neural synchronization, as discussed by Buehlman and Deco [7], where they proposed that synchronization works to optimize the information transfer. Previous results of simulations in the cat cortex showed that the synchronization process depends on the topological structure [8]. In monkeys, it was observed synchronization at gamma-frequency (35 to 90 Hz) when the cortex received proper stimulus [9]. According to measurements in monkeys motor cortex, during a task, neural ensembles can be synchronized at specific frequency bands [10]. In humans, EEG measures have revealed that synchronization of neural activity can be associated with conscious and perception [11]. Synchronization in human cortex has also been observed at the visual cortex, parietal and motor cortex [12]. Parameter spaces for the synchronization in the human connectome was done in [13]. There are works that simulate neural networks with the connectome topology [14,15].

Synchronization can occur in neural ensembles and, in some cases, has been related to pathological rhythms and illnesses, as Parkinson's disease [16,17]. Individuals with Parkinson's disease can exhibit excessive synchronization in the *Globus Pallidus*, leading to movement impairments [18]. According to Silberstein et al. [19], synchronization between cortical areas can be correlated with parkinsonism. One possibility to treat Parkinson's disease is the suppression of synchronization [20].

In this work, we propose a network of networks model based on a real structural connection matrix of human brain to study the synchronization effects. The network describes structural properties of the human cerebral cortex, and the data was kindly provided by Lo et al. [21]. In this network, the cerebral cortex was separated into 78 cortical areas by means of the Automated Anatomical Labeling (AAL) [22]. Every cortical area is represented by one site, the links between sites are proportional to the number of fibers between cortical areas and they were determined through diffusion MRI tractography methods [23]. In our model, each site consists of a network composed of coupled neurons with small-world properties (cortical network). Small-world networks are characterized by a short path length distance between neurons and high local clustering [24,25]. Many neural ensembles have been demonstrated small-world properties, such as the worm *C. Elegans* [24], cortical connection matrices of cats and monkeys [25,26]. Evidences suggesting that structural human brain cortex has small-world properties were found through MRI measures [27,28]. In addition, small-world structures has also been found at cortical columns in the human brain [29].

As local dynamics of the neuron we consider the two-dimensional map proposed by Rulkov [30]. This phenomenological model exhibits many neural dynamical features, like regular spike, burst, and chaotic spikes. These features are generated through the interplay between a fast and a slow variable [31,32]. This model has the advantage of being easy to implement numerically and it has good agreement with experimental results about neural synchronization [33,34].

One of our main results is to show that for the same anatomical neural network, the human cortex can present a huge amount of different complex functional structures as synaptic strength is varied. Moreover, we also show that a delayed feedback signal is efficient to suppress synchronous behavior in our network model.

The structure of the paper is the following: In the Section 2, we introduce our model of neural network and the local dynamics. Each cortical area is defined as one network, the networks are coupled to each other creating a network of networks structure (cortex network). The local dynamics is characterized by bursting activity. In Section 3, we present how to define a geometric phase to study phase synchronization, and how the Kuramoto order parameter can be used to quantify synchronization. In Section 4, we show the effects of suppression of synchronization for the proposed network. In Section 5, we present our conclusions and final remarks.

2. Network of networks model

2.1. Cortex network

The human structural connection matrix used in this work was constructed and kindly provided by Lo et al. [21]. A series of procedures must be done to build the structural network. First, Diffusion Weighted Images [35] are generated from MR measures, after several processes like image registration, spatial normalization and customized template creation, then a 78×78 weighted adjacency matrix W_{ij} is created. The weight in the matrix is determined according to the number of fibers and the fractional anisotropy. The number of fibers was determined using the Fiber Assignment by Continuous Tracking Algorithm [36]. Further details can be found in [21].

For the cortex network we consider the weight W_{ij} as the number of fibers between the cortical areas i and j (Fig. 1). We redefine the weight values (Fig. 1): 0 (white dots), 1 (red dots), 2 (blue dots), and 3 (black dots), where they are distributed by frequency of the interconnected fibers. This selection is to build a connectivity matrix with a heterogeneity less than the real human structural connection matrix.

The degree strength s_i [37], that provides the links intensity for each cortical area in terms of the weight, is given by

$$s_i = \sum_{j=1}^{P} W_{ij}, \tag{1}$$

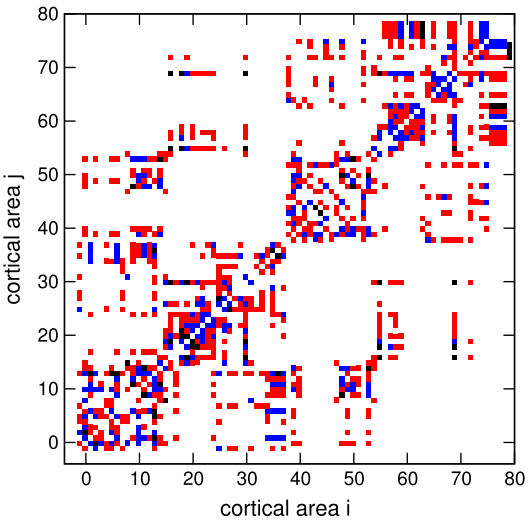

Fig. 1. Weighted adjacency matrix W_{ij} based on a real human structural connection matrix. Colors are set according with the weight: red for 1, blue for 2 and black for 3. (For interpretation of the references to color in this figure legend, the reader is referred to the web version of this article.)

for this case $P = 78$. For the matrix of Fig. 1, the maximum degree strength $s_{\max} = s_{70}$ is equal to 47 and the average degree strength $\langle s \rangle$ is equal to 18.

We also calculate the Cluster Coefficient C and the Path Length L of the network. When two distinct cortical areas j and k are connected to the cortical area i, and also connected between themselves they form a triplet with i. The weight of each triplet is given by the sum: $W_{ij} + W_{ik} + W_{jk}$. The cluster coefficient for each area C_i is the sum of all the triplets related to i divided by the value of the maximum triplet of the network [38]. For weighted matrices, the Path Length L can be evaluated by the average over the sum of the inverse of all minimum paths l_{ij} of the network [39]. For this network, we obtain $C = 0.28$ and $L = 1.65$.

2.2. Local dynamics

The individual dynamics of each neuron in the network is described by the Rulkov model [30]. In this phenomenological model, the neural activity is given by a two-dimensional map with a fast (x) and a slow variable (y),

$$x_{n+1} = \frac{\alpha}{(1 + (x_n^2))} + y_n \tag{2}$$

$$y_{n+1} = y_n - \sigma(x_n - \rho), \tag{3}$$

where α is the bifurcation parameter, $\sigma = 0.001$ and $\rho = -1$. Fig. 2 shows the time evolution of the variables x (black) and y (red).

2.3. Cortical network

We consider that each cortical area is composed of a small world network [24] with 100 neurons. The neurons in the cortical network are connected to their first neighbors (local connections) and have 10% of probability to perform non-local connections inside the network [40]. The cortical networks are coupled to each other and the number of links between each pair of cortical networks is given by the weight in the adjacency matrix: if $W_{ij} = 1$ then there are 50 links between the cortical areas i and j, if $W_{ij} = 2$ then there are 100 links and $W_{ij} = 3$ indicates 150 links. The network has 25% of inhibitory and 75% of excitatory connections [41]. The dynamics of each neuron in the network is given by

$$x_{n+1}^{(l,p)} = \frac{\alpha(l,p)}{(1 + (x_n^{(l,p)})^2)} + y_n^{(l,p)} + \frac{\varepsilon_e}{2}(x_n^{(l-1,p)} + x_n^{(l+1,p)} - 2x_n^{(l,p)}) - \varepsilon_c \sum_{d=1}^{Q} \sum_{f=1}^{P} [T_{(d,f),(l,p)} H(x_n^{(d,f)} - \theta)(x_n^{(l,p)} - V_s)], \tag{4}$$

$$y_{n+1}^{(l,p)} = y_n^{(l,p)} - \sigma(x_n^{(l,p)} - \rho), \tag{5}$$

$$V_s = \begin{cases} 1 & \text{for excitatory connections} \\ -2 & \text{for inhibitory connections,} \end{cases} \tag{6}$$

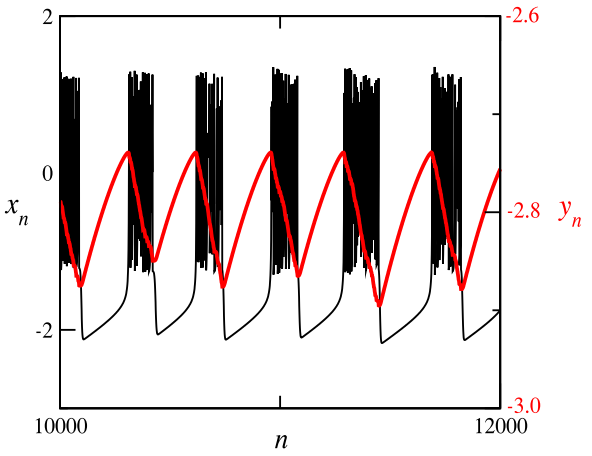

Fig. 2. Example of bursting oscillations produced by the Rulkov model for $\alpha = 4.1$. The black and red colors represent the variables x and y, respectively. (For interpretation of the references to color in this figure legend, the reader is referred to the web version of this article.)

where the index l labels the neuron inside the cortical network and the index p labels the cortex area. $T_{(d,f),(l,s)}$ is the weighted adjacency matrix relating two arbitrary neurons in the network, namely a particular tensor that provides the connectivity between the neurons inside each area and between different areas. $H(x)$ is the Heaviside function, where $\theta = -1$ is the presynaptic threshold for the chemical synapse. The third term in Eq. (4) refers to the local connections, that corresponds to the electrical coupling. This coupling is between the first-neighbors $x_n^{(l-1,p)}$ and $x_n^{(l+1,p)}$ inside each cortex area, where the neurons are on a ring. The fourth term refers to the non-local connections, that can be associated with chemical coupling. The chemical couplings occur between neurons inside each cortex area and between neurons in different areas. This way, the topology of the neurons inside each area has small-world property. We define ε_e as the electrical coupling strength and ε_c as the chemical coupling strength [40]. The parameter $\alpha(l, p)$ is uniformly sorted from the interval [4.1:4.3] (generating square burstings) [30], $P = 78$ and $Q = 100$.

3. Phase synchronization

The time series of a Rulkov neuron (Eqs. (2) and (3)) is shown in Fig. 2. Each time that a burst ignites the y variable reaches a maximum value (red line in Fig. 2). Based on this fact, we define a phase φ considering the maximum values of y such that

$$\varphi_n = 2\pi k + 2\pi \frac{n - n_k}{n_{k+1} - n_k}, \tag{7}$$

where n_k is the ignition time of the kth burst [42].

When the electrical (ε_e) and chemical (ε_c) coupling strength are changed properly, the neurons can exhibit phase synchronization. The phase synchronization can be identified through the Kuramoto order parameter [43] and its time evolution is given by

$$r_n = \frac{1}{K}\left|\sum_{k=1}^{K} e^{i\varphi_n^{(k)}}\right|, \tag{8}$$

where K is the number of neurons. We calculate the time average order parameter $\bar{R}$, that is given by

$$\bar{R} = \frac{1}{n'}\sum_{n=1}^{n'} r_n, \tag{9}$$

where n' is a large number of iterations. When the order parameter is 1 the set of neurons is fully synchronized, when the order parameter is 0 then the set of neurons is fully asynchronous. If we intend to measure the time average order parameter for the whole cortex network ($\bar{R}$), then the sum is over all the neurons in the network, i.e., $K = QP$, and the k index is replaced to $k = (l, p)$. The synchronization in the cortical networks ($\bar{R}_p$) can be analyzed when p index is fixed and the sum is over all neurons of the cortical network, in this case, $K = Q$ and $k = (l, p)$. The synchronization between pairs of cortical networks ($\bar{R}_{pp'}$) is calculated if two p values are selected and the sum is over all neurons of the two networks, such that $K = 2Q$.

When the electrical coupling strength is held constant ($\varepsilon_e = 0.005$) the cortex network starts to exhibit partial phase synchronization ($\bar{R} > 0.5$) after the chemical coupling strength is increased above $\varepsilon_c = 0.001$, as shown in Fig. 3. Some cortical networks can be internally more synchronized than others, for example the cortical network 16 (blue line) is more

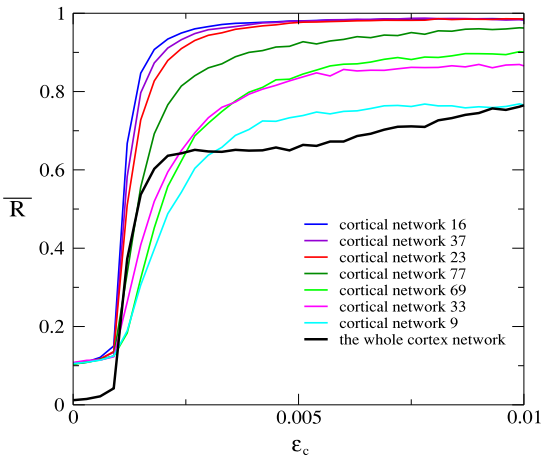

Fig. 3. Time average order parameter for the whole cortex network and some selected cortical networks for $\varepsilon_e = 0.005$. The average is defined over 50 distinct set of initial conditions and 10 000 iterations after 80 000 transient iterations. The cortical networks 9, 16, 23, 33, 37, 69, 77 have degrees equal to 13, 21, 23, 4, 18, 18, and 19, respectively. (For interpretation of the references to color in this figure legend, the reader is referred to the web version of this article.)

synchronized than the cortical network 9 (cyan line). For $\varepsilon_c = 0.0099$, the cortical areas with smaller degree strength s_i are the areas with less synchronization. Surprisingly, the areas with highest synchronization are not those with largest degree strength s_p.

After the onset of phase synchronization ($\varepsilon_c > 0.001$) some areas may synchronize to each other. The time average order parameter between all the cortical networks for different values of chemical coupling strength ε_c is shown in Fig. 4. Blue and Purple lines indicate the pairs of cortical networks that are not synchronized to each other, yellow and green lines indicate those synchronized. As the chemical coupling strength ε_c is increased we observe that more areas synchronize to each other. We consider that two areas are mutually synchronized above a certain threshold value of $\bar{R}$. Here we consider as threshold a value greater than 0.6. When $\varepsilon_c = 0.0015$ the areas with more mutual synchronization in number of areas are those with largest degree strength s_p. However, for $\varepsilon_c = 0.005$ the same fact is not observed. As the chemical coupling strength ε_c varies the number of cortical areas synchronized can change.

4. Suppression

People suffering of parkinsonism can exhibit excessive synchronization in the brain, synchronization in this cases are related to movement impairments [18]. One strategy to avoid or relieve these symptoms is to apply a delayed feedback signal in the cortical areas to suppress the synchronization [44]. As each cortical area is described by a different network, the delayed feedback control $M(\tau, p)$ associated with a specific cortical network p is defined as

$$M_n(\tau, p) = \frac{1}{Q}\sum_{l=1}^{Q} x_{n-\tau}^{(l,p)}, \tag{10}$$

where τ is the time delay. In this case, to suppress the synchronization a delayed signal is introduced in the fast variable x of all neurons in the cortical network p. The fast variable is then modify to

$$\begin{aligned} x_{n+1}^{(l,p)} = {} & \frac{\alpha(l,p)}{(1+(x_n^{(l,p)})^2)} + y_n^{(l,p)} + \frac{\varepsilon_e}{2}(x_n^{(l-1,p)} + x_n^{(l+1,p)} - (2x_n^{(l,p)})) \\ & - \varepsilon_c \sum_{d=1}^{Q}\sum_{f=1}^{P}[T_{(d,f),(l,p)}H(x_n^{(d,f)} - \theta)(x_n^{(l,p)} - V_s)] + \varepsilon_F M_n(\tau, p), \end{aligned} \tag{11}$$

where ε_F is the intensity of the delayed signal. The success of such strategy can be verify by means of the suppression factor S [45], that is given by

$$S = \sqrt{\frac{\mathrm{Var}(M)}{\mathrm{Var}(M(\tau, p))}}, \tag{12}$$

where M is the mean field in the absence of feedback inputs and Var() is the variance. The synchronization suppression is achieved when $S \gg 1$.

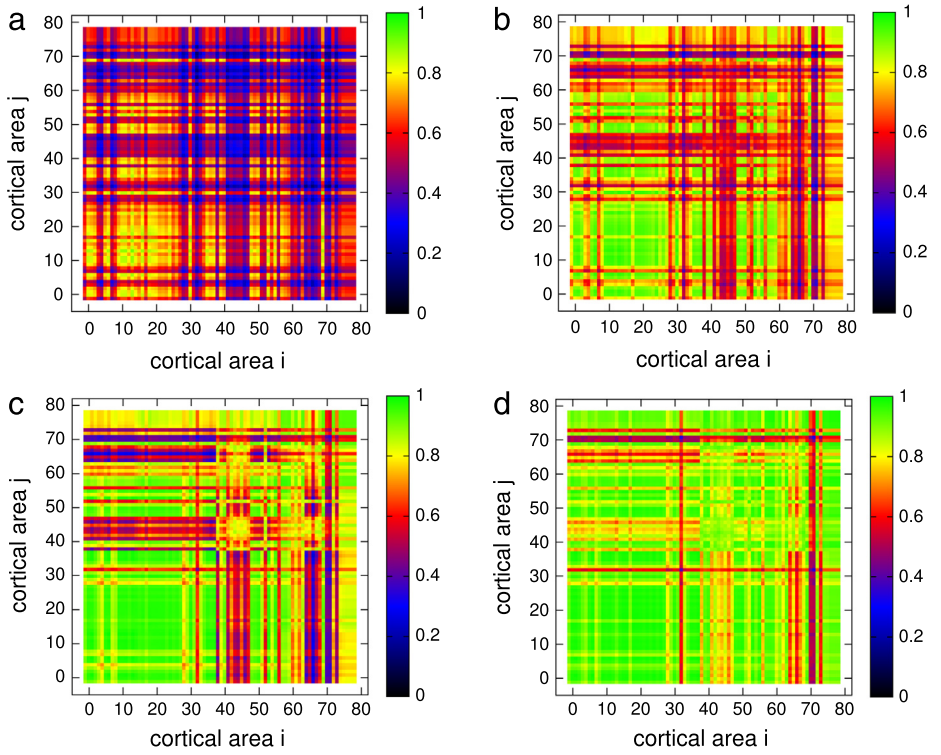

Fig. 4. Time average order parameter (color bar) between all the cortical networks for $\varepsilon_e = 0.005$, (a) $\varepsilon_c = 0.0015$, (b) $\varepsilon_c = 0.0025$, (c) $\varepsilon_c = 0.005$, and (d) $\varepsilon_c = 0.01$. The average is calculated over 10 000 iterations after 80 000 transient iterations. (For interpretation of the references to color in this figure legend, the reader is referred to the web version of this article.)

There is no certainty that applying a feedback signal into a synchronized network will enhance or weaken the synchronization. Usually, the parameter space $\varepsilon_F \times \tau$ exhibits some regions, called "tongues", where the suppression factor S is greater than one. These tongues represent the region of the parameter space where the delayed feedback control is effective in the suppression of synchronization [45].

In our case, when the feedback signal is applied in one cortical network, no tongues are observed. For this reason, we analyze the situation where 25%, 50%, 75% and 100% of the cortical networks are perturbed with delayed signals in order to verify if the suppression strategy is efficient, as shown in Fig. 5. Each cortical network is perturbed with a different signal produced by its own delayed mean field. In Fig. 5, the suppression factor S of all cortical networks are showed for each (ε_F, τ) in color scale. When more cortical networks are perturbed, higher is the suppression factor S, besides, smaller is the size of the tongue. Moreover, when 25% of the cortical networks are perturbed the tongue is large, it spreads through the parameter space and its limits are difficult to define. When all the cortical networks are perturbed it is easy to define the tongue. Depending on the number of suppressed cortical networks the center of the tongue is displaced.

We calculate the average order parameter between all the cortical networks with a delayed feedback signal, in order to get a better understanding about the effectiveness of the feedback signal strategy. We apply a feedback signal in 25% of the cortical networks considering the same parameters used in Fig. 4(c). Fig. 6(a) exhibits a case in that the feedback signal, for $\tau = 145$ and $\varepsilon_F = 0.01$, is not able to suppress synchronous behavior. The success of the feedback signal to suppress the synchronization occurs when we consider $\tau = 145$ and $\varepsilon_F = 0.035$, as shown in Fig. 6(b).

5. Conclusions

We present a model of network of networks, where cortical areas are represented by networks composed of coupled Rulkov neurons. In our simulations, we observe that when the chemical coupling strength ε_c increases the system evolves to a stable partial synchronized state. Despite of this fact, the intensity of phase synchronization between the cortical areas varies depending on ε_c. This result indicates that for the same structural connection matrix a huge amount of dynamical patterns can emerge in the network.

Neural synchronous behavior can be associated with brain disorders. Due to this fact, we use the delay feedback control as a method of suppression of phase synchronization. As a result, we verify that it is necessary to perturb more than one cortical network to suppress the synchronization. Our simulations show that increasing the number of perturbed cortical networks the tongue size decreases and the suppression factor S increases.

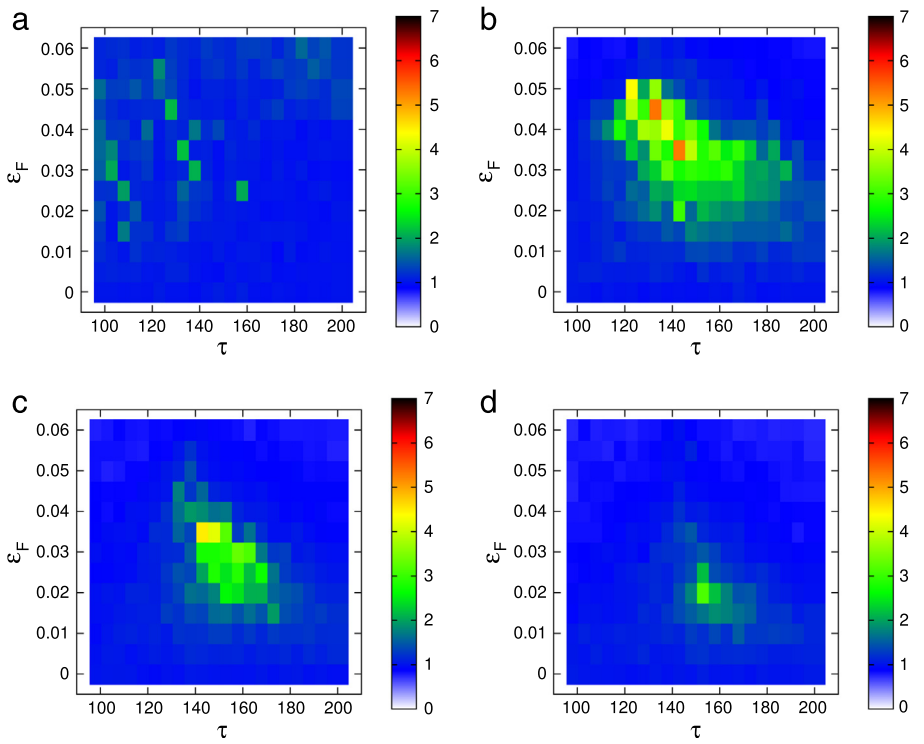

Fig. 5. Suppression factor S (color bar) as function of the delayed signal intensity ε_F and time delay τ. Percentage of the perturbed cortical networks: (a) 25%, (b) 50%, (c) 75%, and (d) 100%. (For interpretation of the references to color in this figure legend, the reader is referred to the web version of this article.)

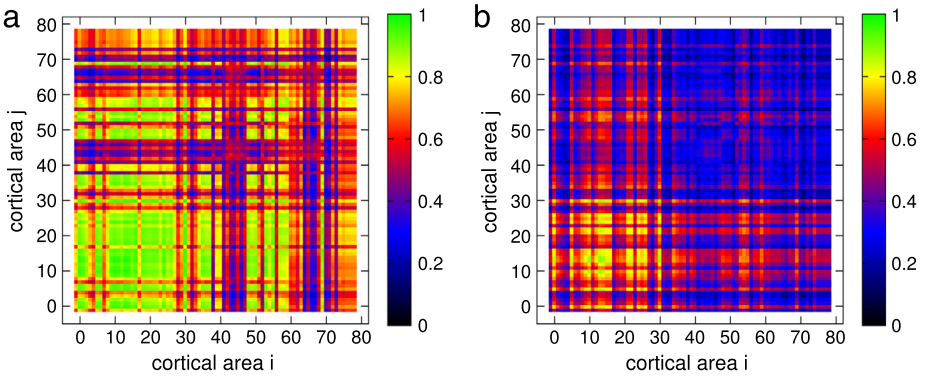

Fig. 6. Time average order parameter (color bar) between all the cortical networks for $\varepsilon_e = 0.005$, $\varepsilon_c = 0.005$, $\tau = 145$, (a) $\varepsilon_F = 0.01$, and (b) $\varepsilon_F = 0.035$. (For interpretation of the references to color in this figure legend, the reader is referred to the web version of this article.)

Our results suggest that for external perturbation in real brains, people should find a balance between the number of perturbed areas and signal properties (intensity and time delay) in order to find the settings where suppression is successful.

We observed finite values for the time average order parameter. These values suggest that the network for weak coupling values could present the phenomenon "Collective Almost Synchronization" [46]. We observed that the value of the synchronization suppression is larger on some areas than others. Even though, we did not find a relation between the variance of the mean field and the degree neither at cortex network nor cortical network level. More analysis are necessary to confirm or deny the existence of Collective Almost Synchronization in our network, we plan to investigate the reason for this behavior in future works.

Acknowledgments

This study was possible by partial financial support from the following agencies: Fundação Araucária, Brazilian National Council for Scientific and Technological Development (CNPq), Coordination for the Improvement of Higher Education Personnel (CAPES), and São Paulo Research Foundation (FAPESP) process numbers 2015/07311-7, 2011/19296-1, and 2017/20920-8.

References

[1] E.R. Kandel, J.H. Schwartz, T.M. Jessell, Principles of Neural Science, McGraw-Hill Companies, Inc., New York, 2000.
[2] S. Shipp, Structure and function of the cerebral cortex, Curr. Biol. 17 (2007) 443–449.
[3] E. Bullmore, O. Sporns, Complex brain networks: graph theoretical analysis of structural and functional systems, Nat. Rev. Neurosci. 10 (2009) 186–198.
[4] G. Zamora-López, C. Zhow, J. Kurths, Exploring brain function from anatomical connectivity, Front. Neurosci. 5 (2011) 1–11.
[5] G. Zamora.-López, Y. Chen, G. Dec, M.L. Kringelbach, C. Zhou, Functional complexity emerging from anatomical constraints in the brain: the significance of network modularity and rich-clubs, Sci. Rep. 6 (2016) 1–18.
[6] R.D. Traub, M.A. Whittington, I.M. Stanford, J.G.R. Jefferys, A mechanism for generation of long-range synhronous fast oscillations in the cortex, Nature 383 (1996) 621–624.
[7] A. Buehlmann, G. Deco, Optimal information transfer in the cortex through synchronization, PLoS Comput. Biol. 6 (2010) e100934.
[8] J. Gómez-Gardeñes, G. Zamora-López, Y. Moreno, A. Arenas, From modular to centralized organization of synchronization in functional areas of the cat cerebral cortex, PLoS One 5 (2010) e12313.
[9] P. Fries, J.H. Reynolds, A.E. Rorie, R. Desimone, Modulation of oscillatory neuronal synchronization by selective visual attention, Science 291 (2001) 1560–1563.
[10] S.N. Baker, R. Spinks, A. Jackson, R.N. Lemon, Synchronization in monkey motor cortex during a precision grip task. Task-Dependent Modulation in Single-Unit Synchrony, J. Neurophysiol. 85 (2001) 869–885.
[11] L. Melloni, C. Molina, M. Pen, D. Torres, W. Singer, E. Rodriguez, Synchronization of neural activity across cortical areas correlates with conscious perception, J. Neurosci. 27 (2007) 2858–2865.
[12] P.R. Roelfsema, A.K. Engel, P. König, W. Singer, Visuomotor integration is associated with zero time-lag synchronization among cortical areas, Nature 385 (1997) 157–161.
[13] C.G. Antonopoulos, S. Srivastava, S.E.S. Pinto, M.S. Baptista, Do brain networks evolve by maximizing their information flow capacity? PLoS Comput. Biol. 11 (2015) e1004372.
[14] L.K. Gallos, H.A. Markse, M. Sigman, A small world of weak ties provides optimal global integration of self-similar modules in functional brain networks, Proc. Natl. Acad. Sci. USA 109 (2012) 2825–2830.
[15] M.S. Baptista, R.M. Szmoski, R.F. Pereira, S.E.S. Pinto, Chaotic, informational and synchronous behaviour of multiplex networks, Sci. Rep. 6 (2016) 22617.
[16] M.G. Rosenblum, A.S. Pikovsky, Delayed feedback control of collective synchrony: An approach to suppression of pathological brain rhythms, Phys. Rev. E 70 (2004) 041904.
[17] L. Timmermann, J. Gross, M. Dirks, J. Volkmann, H.J. Freund, A. Schnitzler, The cerebral oscillatory network of parkinsonian resting tremor, Brain 126 (2003) 199–212.
[18] D.S. Andres, F. Gomez, F.A.S. Ferrari, D. Cerquetti, M. Merello, R.L. Viana, R. Stoop, Multiple-time-scale framework for understanding the progression of Parkinson's disease, Phys. Rev. E 90 (2014) 062709.
[19] P. Silberstein, A. Pogosyan, A.A. Kühn, G. Hotton, S. Tisch, A. Kupsch, P. Dowsey-Limousin, M.I. Hariz, P. Brown, Cortico-cortical coupling in Parkinson's disease and its modulation by therapy, Brain 128 (2005) 1277–1291.
[20] C. Hammond, H. Bergman, P. Brown, Pathological synchronization in Parkinson's disease: networks, models and treatments, Trends Neurosci. 30 (2007) 357–364.
[21] C.-Y. Lo, P.-N. Wang, K.-H. Chou, J. Wang, Y. He, C.-P. Lin, Diffusion tensor tractography reveals abnormal topological organization in structural cortical networks in alzheimer's disease, J. Neurosci. 15 (2010) 16876–16885.
[22] N. Tzourio-Mazoyer, B. Landeau, B. Papathanassiou, F. Crivello, O. Etard, N. Delcroix, B. Mazoyer, M. Joliot, Technical note: Automated anatomical labeling of activations in spm using a macroscopic anatomical parcellation of the mni mri single-subject brain, Neuroimage 15 (2002) 273–289.
[23] B.J. Jellison, A.S. Field, J. Medow, M. Lazar, M.S. Salamat, A.L. Alexander, Diffusion tensor imaging of cerebral white matter: a pictorial review of physics, fiber tract anatomy, and tumor imaging patterns, Am. J. Neuroradiol. 25 (2004) 356–369.
[24] D.J. Watts, S.H. Strogatz, Collective dynamics of 'small-world' networks, Nature 393 (1998) 440–442.
[25] D.S. Bassett, E.D. Bullmore, Small-world brain networks, Neurosci. 12 (2006) 512–523.
[26] O. Sporns, J.D. Zwi, The small world of the cerebral cortex, Neuroinformatics 2 (2004) 145–162.
[27] Y. He, Z.J. Chen, A.C. Evans, Small-world anatomical networks in the human brain revealed by cortical thickness from MRI, Cerebral Cortex 17 (2007) 2407–2419.
[28] C.J. Stam, E.C.W. van Straten, The organization of physiological brain networks, Clin. Neurophysiol. 123 (2012) 1067–1087.
[29] R. Stoop, V. Saase, C. Wagner, B. Stoop, R. Stoop, Beyond scale-free small-world networks: cortical columns for quick brains, Phys. Rev. Lett. 110 (2013) 108105.
[30] N.F. Rulkov, Regularization of synchronized chaotic bursts, Phys. Rev. Lett. 86 (2001) 183–186.
[31] G. de Vries, Bursting as an emergent phenomenon in coupled chaotic maps, Phys. Rev. E 64 (2001) 051914.
[32] H. Chen, J. Zhang, J. Liu, Enhancement of neuronal coherence by diversity in coupled Rulkov-map models, Physica A 387 (2008) 1071–1076.
[33] R.C. Elson, A.I. Selverston, R. Huerta, N.F. Rulkov, M.I. Rabinovich, H.D.I. Abarbanel, Synchronous behavior of two coupled biological neurons, Phys. Rev. Lett. 81 (1998) 5692–5695.
[34] P. Varona, J.J. Torres, H.D.I. Abarbanel, M.I. Rabinovich, R.C. Elson, Dynamics of two electrically coupled chaotic neurons: Experimental observations and model analysis, Biol. Cybernet. 84 (2001) 91–101.
[35] C. Pierpaoli, P. Jezzard, P.J. Basser, A. Barnett, G. Di Chiro, Diffusion Tensor MR Imaging of the Human Brain, Radiology 201 (1996) 637–648.
[36] F. Christidi, E. Karavasilis, K. Samiotis, S. Bisdas, N. Papanikolaou, Fiber tracking: A qualitative and quantitative comparison between four different software tools on the reconstruction of major white matter tracts, Eur. J. Radiol. Open 3 (2016) 153–161.
[37] A. Barrat, M. Barthélemy, R. Pastor-Satorras, A. Vespignani, The architecture of complex weighted networks, Proc. Natl. Acad. Sci. USA 101 (2004) 3747–3752.
[38] T. Opsahl, P. Panzarasa, Clustering in weighted networks, Social Networks 31 (2009) 155–163.
[39] T. Opsahl, F. Agneessens, J. Skvoretz, Node centrality in weighted networks: Generalizing degree and shortest paths, Social Networks 32 (2010) 245–251.

[40] E.L. Lameu, F.S. Borges, R.R. Borges, K.C. Iarosz, I.L. Caldas, A.M. Batista, R.L. Viana, J. Kurths, Suppression of phase synchronisation in network based on cat's brain, Chaos 26 (2016) 043107.
[41] T.W. Lee, Network Balance and Its Relevance To Affective Disorders: Dialetic Neuroscience, Pronoun, New York, 2016.
[42] M.V. Ivanchenko, G.V. Osipov, V.D. Shalfeev, J. Kurths, Phase synchronization in ensembles of bursting oscillators, Phys. Rev. Lett. 93 (2004) 134101.
[43] Y. Kuramoto, Self-entrainment of a population of coupled non-linear oscillators, Lecture Notes in Phys. 39 (1975) 420–422.
[44] C.A.S. Batista, S.R. Lopes, R.L. Viana, A.M. Batista, Delayed feedback control of bursting synchronization in a scale-free neuronal network, Neural Netw. 23 (2010) 114–124.
[45] M.G. Rosenblum, A.S. Pikovsky, Controlling synchronization in an ensemble of globally coupled oscillators, Phys. Rev. Lett. 92 (2004) 114102.
[46] M.S. Baptista, H.-P. Ren, J.C.M. Swarts, R. Carareto, H. Nijmeijer, C. Grebogi, Collective almost synchronisation in complex networks, PLoS One 7 (2012) e48118.